

1 **A SIMPLE PARTICLE SIZE DISTRIBUTION MODEL FOR GRANULAR MATERIALS**

2
3 Chen-Xi Tong^{1,2}, Glen J. Burton¹, Sheng Zhang^{2*}, Daichao Sheng^{1,2}

4 1. ARC Centre of Excellence for Geotechnical Science and Engineering, The University of
5 Newcastle, Callaghan, NSW 2308, Australia

6 2. National Engineering Laboratory for High-Speed Railway Construction, Central South
7 University, Changsha, 410075, China

8
9
10
11
12
13 * corresponding author

14 PhD Professor Sheng Zhang

15 National Engineering Laboratory for High-Speed Railway Construction, Central South
16 University, Changsha, 410075

17 P.R. China

18 Mobile: +8613907315427

19
20
21
22
23
24
25

26 ABSTRACT: Particle size distribution (PSD) is a fundamental soil property that plays an
27 important role in soil classification and soil hydro-mechanical behaviour. A continuous
28 mathematical model representing the PSD curve facilitates the quantification of particle
29 breakage, which often takes place when granular soils are compressed or sheared. This paper
30 proposes a simple and continuous PSD model for granular soils involving particle breakage. The
31 model has two parameters and is able to represent different types of continuous PSD curves. It is
32 found that one model parameter is closely related to the coefficient of non-uniformity (C_u) and
33 the coefficient of curvature (C_c), while the other represents a characteristic particle diameter. A
34 database of 53 granular soils with 154 varying PSD curves are analyzed to evaluate the
35 performance of the proposed PSD model, as well as three other PSD models in the literature. The
36 results show that the proposed model has improved overall performance and captures the typical
37 trends in PSD evolution during particle breakage. In addition, the proposed model is also used
38 for assessing the internal stability of 27 widely graded soils.

39

40 Keywords: granular soil; PSD; mathematical model; particle breakage; internal stability

41

42

43

44

45

46

47

48

49

50

51

52

53

54

55

56 INTRODUCTION

57 Particle size distribution (PSD) is a basic soil property and the main basis for soil classification.
58 It is used in analysis of stability of granular filters (Kenney and Lau 1985; Åberg 1993;
59 Indraratna et al. 2007), internal instability and suffusion of granular soils (Wan and Fell, 2008;
60 Indraratna et al. 2015; Moraci et al. 2014, 2015; Ouyang and Takahashi 2016a, 2016b),
61 groutability of soils (Karol 1990; Vipulanandan and Ozgurel 2009; EI Mohtar et al. 2015), soil-
62 water characteristic curves (Fredlund et al. 2002; Gallage and Uchimura 2010), and debris flow
63 (Sanvitale and Bowman 2017). Particle size distribution curves are widely used to represent soil
64 composition in real engineering practice and academic research. Particle size distribution curves
65 can be obtained by sieving test, where several constrained grain sizes are predetermined. At
66 present, indices such as the coefficient of uniformity C_u and the coefficient of curvature C_c are
67 usually used to evaluate the whole gradation of a soil. For example, the standard for engineering
68 classification of soils in China (GB/T50145-2007) suggest that the soil is well graded when $C_u > 5$
69 and $1 \leq C_c \leq 3$; otherwise, the soil is poorly graded. However, neither C_u or C_c can describe a PSD
70 curve completely, as no unique relation exists between these coefficients and a PSD curve.

71
72 Another important application of studying the PSD lies in studying particle breakage of granular
73 soils. A large number of studies have shown that soil particles, especially coarse-grained soil
74 particles, can break under loading (Lee and Farhoomand 1967; Marsal 1967; Hardin 1985;
75 Zheng and Tannant 2016; Hyodo et al. 2017). Some trends have been highlighted when particles
76 break (Mayoraz et al. 2006; Altuhafi and Coop 2011; Miao and Airey 2013), for example, there
77 seems to be an ultimate fractal PSD according to a large number of studies in the literature
78 (Sammis et al. 1987; McDowell et al. 1996; Einav 2007). The three key elements in studying the
79 behaviour of a soil that involves particle breakage are: (1) a simple and adequate representation
80 of an evolving PSD, (2) the evolution of the PSD under various stresses and strains, and (3) the
81 correlation between the PSD and soil hydro-mechanical properties (Muir Wood and Maeda 2008;
82 Zhang et al. 2015). The first element is the foundation for studying the second and third
83 elements, and is the purpose of this study. The second element is studied in Einav (2007), Zhang
84 et al. (2015) and others, while the third element is an area of future interest. In the literature,
85 studies on PSD representation (first element) and PSD evolution (second element) are usually
86 carried out separately, often by different researchers from different backgrounds. However, it

87 will be shown in this paper that these two are somewhat related for soils subjected to particle
88 breakage.

89
90 While there are simple quantitative representations of soil PSDs in the literature (for example, C_c
91 and C_u), an alternative way to describe a PSD curve is perhaps to adopt a suitable mathematical
92 model which covers the full range of particle sizes. Such a mathematical model has several
93 advantages: (1) characteristics of the whole PSD curve (such as d_{10} , d_{60} , C_c , C_u , etc.) can be
94 obtained when the parameters of the model are determined; (2) it is easier to correlate the entire
95 PSD curve with other properties of the soil. A key challenge is in developing a model that has a
96 limited number of parameters while still capturing the widely varying nature of soil PSDs. In the
97 case of particle breakage, the PSD model should ideally be able to predict the evolution of the
98 grading.

99
100 A number of studies have attempted to characterize PSD curves using mathematical models, with
101 up to seven input parameters. The most commonly used PSD model is perhaps the Gates-
102 Gaudin-Schuhmann model (GGSM) (Schuhmann 1940), which was previously proposed by
103 Fuller (Fuller and Thompson 1907) and Talbot (Talbot and Richart 1923):

$$104 \quad P(d) = \left(\frac{d}{d_{\max}}\right)^m, \quad 0 < d < d_{\max} \quad (1)$$

105 where parameter m is a fitting parameter, d_{\max} is the diameter of the largest particle; $P(d)$ is the
106 mass percentage of particles passing a particular size d . Equation (1) has the same form with
107 Fractal Models (FM) in the literature (Turcotte 1986; Einav 2007). In a Fractal Model, parameter
108 m equals $3-D$, with D being the fractal dimension of the soil specimen. For a uniformly graded
109 soil, the PSD is not fractal, but we can still use an appropriate D value to describe the PSD. In
110 this case, D is not the fractal dimension, but a fitting parameter. However, with particle breakage,
111 the PSD tends to become more and more fractal, and therefore D is usually called the fractal
112 dimension.

113
114 Another widely-used one-parameter model is the Gaudin-Melog model (GMM) proposed by
115 Harris (1968):

$$P(d)=1-\left(1-\frac{d}{d_{\max}}\right)^k, \quad 0 < d < d_{\max} \quad (2)$$

where k is a fitting parameter.

Equations (1) and (2) are perhaps the simplest mathematical representations of a PSD. They have one fitting parameter and one specific particle size (d_{\max}). Other models in the literature can have as many as two to seven fitting parameters (Vipulanandan and Ozgurel 2009; Fredlund et al. 2000). A widely used model for well-graded soils is the Fredlund unimodal model (FUM) (Fredlund et al. 2000):

$$P(d)=\frac{1}{\left\{\ln\left[\exp(1)+\left(\frac{a_{gr}}{d}\right)^{n_{gr}}\right]\right\}^{m_{gr}}}\left\{1-\frac{\left[\ln\left(1+\frac{d_{rgr}}{d}\right)\right]^7}{\left[\ln\left(1+\frac{d_{rgr}}{d_m}\right)\right]^7}\right\} \quad (3)$$

where d_m is the minimum size particle and a_{gr} , n_{gr} , m_{gr} and d_{rgr} are the four fitting parameters: a_{gr} defines the inflection point, n_{gr} the uniformity of the PSD (i.e. steepness of the PSD), m_{gr} the shape of the curve at small particle sizes and d_{rgr} is related to the amount of fines.

The performance of the different models have been previously compared against experimental data (Hwang et.al. 2002; Merkus 2009; Vipulanandan and Ozgurel 2009; Luo et.al. 2014; Bayat et.al. 2015; Zhou et.al. 2016). In general, a model with more parameters leads to better fitting of the experimental results. Models currently in the literature are used to fit specific PSD curves, not necessarily an evolving PSD curve due to particle breakage. The evolution of PSD during particle breakage follows certain trends, which are more identifiable for an initially uniformly graded soil specimen (Zhang et al. 2015), and the capacity of existing models in predicting an evolving PSD curve remains unclear.

In this paper, a simple two-parameter PSD model for granular soils is proposed based on the studies of particle breakage. The performance of the proposed model and two other simple one-parameter models (GGSM and GMM listed above) and the four-parameter model (FUM) are

141 compared against experimental data obtained for soil specimens involving particle breakage
 142 and . The evolution of model parameters during particle breakage is studied. The proposed PSD
 143 model is also applied to assess the internal stability of widely graded granular soils.

144

145 A SIMPLE PSD MODEL AND DETERMINATION OF ITS PARAMETERS

146 In our previous studies (Zhang et.al. 2015; Tong et.al. 2015), we considered particle breakage as
 147 a probabilistic event, and defined a breakage probability to measure the degree of particle
 148 breakage of a uniformly graded soil sample. A two-parameter Weibull distribution was proposed
 149 to describe the distribution of new particles generated from the breakage (Figure 1). As shown in
 150 Figure 1, the initially uniformly graded soil sample (with particle sizes between $d_{\max-1}$ and d_{\max})
 151 will break by a percentage (p) of the original mass, leading to a Weibull distribution of new
 152 particles (with particle size of $d_1, d_2, \dots, d_{\max-1}$) as Equation 4:

153

$$154 \quad P^* = 1 - e^{-\left[\frac{x_i}{\lambda(1-x_i)}\right]^\kappa} \quad (4)$$

155

156 where P^* is the distribution of new particles generated from the particle breakage of an initially
 157 uniformly graded sample, $x_i = d_i/d_{\max-1}$ is the particle size ratio, d_{\max} is the diameter of the
 158 maximum size particle, and $d_{\max-1}$ is the second largest particle diameter (second largest sieve
 159 size); λ is a scale parameter and κ is a shape parameter. As shown in Zhang et al. (2015), the
 160 main advantage of the proposed Weibull distribution is twofold: (1) it captures particle breakage
 161 of different patterns such as asperity breakage, surface grinding and particle splitting; and (2) it
 162 can be integrated into a Markov chain model to describe the breakage process of a non-uniformly
 163 graded soil sample.

164

165 Equation (4) defines the distribution of new particles, with sizes less than $d_{\max-1}$, generated as a
 166 result of breakage, for example. The PSD of the whole specimen after breakage, is then based on
 167 the breakage probability or the percentage of broken mass (p). The percentages of particles in
 168 different size groups can then be calculated as follows:

$$\begin{cases}
 P(d) = \left\{ 1 - e^{-\left(\frac{\frac{d}{d_{\max-1}}}{\lambda(1-\frac{d}{d_{\max-1}})}\right)^\kappa} \right\} \times p, & 0 < d \leq d_{\max-1} \\
 P(d) = p + \frac{1-p}{d_{\max} - d_{\max-1}} \times (d - d_{\max-1}), & d_{\max-1} < d \leq d_{\max}
 \end{cases} \quad (5)$$

Equation (5) is a two-part function that is not continuously differentiable. It can be treated as a PSD model to some extent. When the size of particles is between 0 and $d_{\max-1}$, $P(d)$ can be calculated from the first part of Equation (5). When the particle size is between $d_{\max-1}$ and d_{\max} , the $P(d)$ can be obtained by linear interpolation as used in the second part of Equation (5). Equation (5) is supposed to describe the PSD of a granular soil of an arbitrary breakage probability (p). For a uniformly graded sample and a zero breakage probability, the PSD of the soil is $P(d)=(d-d_{\max-1})/(d_{\max}-d_{\max-1})$. It represents a line in the $P(d)$ - d space, as shown in Figure 1. It is important to note that for real samples, the second largest particle may not be determined, as the PSD is defined at distinct points. Here, for a uniformly graded sample, the second largest particle size $d_{\max-1}$ is the same as d_{\min} .

The PSD of an initially uniformly graded granular soil after breakage tends to be continuous, or well graded, after breakage (Nakata et al. 2001; Zhang and Baudet 2013). Here, we consider the PSD curve of a granular soil after breakage as a continuous curve, with the second largest particle size $d_{\max-1}$ infinitely approaching the maximum particle size d_{\max} . In this case, the particle breakage probability p approaches 100% as shown in Figure 1. Equation (5) is then reduced to

$$P(d) = \lim_{d_{\max-1} \rightarrow d_{\max}} \left\{ 1 - e^{-\left(\frac{\frac{d}{d_{\max-1}}}{\lambda(1-\frac{d}{d_{\max-1}})}\right)^\kappa} \right\} = 1 - e^{-\left(\frac{d}{\lambda(d_{\max}-d)}\right)^\kappa} \quad (6)$$

Equation (6) is a new PSD model for non-uniformly graded granular soils broken from uniformly graded sample. It is also a modified Weibull distribution model, with two parameters: a scale parameter λ and shape parameter κ . This model reflects the fact that the mass percentage of particles $P(d)$ has a limit value of 1 when passing a particular size d_{\max} . The values of the two parameters can be calculated if two PSD points, such as: $(d_{10}, P(d_{10}))$ and $(d_{60}, P(d_{60}))$ are

192 known. Once the values of the two parameters are determined, the PSD of a granular soil can be
 193 determined uniquely.

194

195 As shown in Equation (6), when $d=\lambda*d_{max}/(1+\lambda)$, the value of $P(d)\equiv 1-1/e\approx 0.632$, irrespective of
 196 κ value. Parameter λ is then determined as

$$197 \quad \lambda = \frac{d_{63.2}}{d_{max} - d_{63.2}} \quad (7)$$

198 where $d_{63.2}$ is the characteristic particle diameter at which 63.2% of the sample by mass is
 199 smaller. Equation (7) is the theoretical solution of parameter λ . It is a non-dimensional parameter
 200 and is only related to characteristic particle diameters $d_{63.2}$ and d_{max} . Substituting Equation (7)
 201 into Equation (6) leads to the final form of the PSD model:

$$202 \quad P(d) = 1 - e^{-\left(\frac{d(d_{max}-d_{63.2})}{d_{63.2}(d_{max}-d)}\right)^\kappa} \quad (8)$$

203 Equation (8) is an exponential function. If the values of d_{max} and parameter λ are known, the
 204 parameter κ can easily be obtained by using MATLAB fitting toolbox (cftool) ([Matlab R2016b](#)).
 205 The performance of the proposed PSD model can be evaluated according to the coefficient of
 206 determination R^2 , defined as following:

$$207 \quad R^2 = 1 - \frac{\sum_1^N (Y_i - Y_j)^2}{\sum_1^N (Y_i - \bar{Y}_i)^2} \quad (9)$$

208 where Y_i and Y_j are actual and calculated cumulative mass of particles finer than d , respectively.
 209 \bar{Y}_i is mean of actual value.

210

211 The flow chart for obtaining and assessing parameter λ and κ is shown in Figure 2. The fitting
 212 process can be summarised as follows:

213 (1) Experimental characteristic diameter $d_{63.2}^*$ is determined by linear interpolation of the
 214 sieving test data.

- 215 (2) Parameter λ is calculated using Equation (7).
- 216 (3) Parameter κ is found by a nonlinear least square fitting of the experimental PSD data,
217 based on the trust-region algorithm method in Matlab.
- 218 (4) The predicted characteristic diameter $d_{63.2}^{\#}$ is determined from Equation (6), and is
219 compared with the experimental characteristic diameter $d_{63.2}^*$.
- 220 (5) Optimal values of λ and κ are obtained only when the coefficient of determination R^2
221 obtained in step 3 is sufficiently large ($R^2 \geq 0.95$) and the difference between the predicted
222 and experimental values of $d_{63.2}$ is sufficiently small ($\Delta d_{63.2} = |d_{63.2}^* - d_{63.2}^{\#}| / d_{63.2}^* \leq 0.01$).
223 Otherwise, the experimental characteristic diameter $d_{63.2}$ is reset to the predicted value and
224 the above steps are repeated.
- 225 (6) The maximum iteration is set to 5. If either $R^2 < 0.95$ or $\Delta d_{63.2} > 0.01$ is satisfied, exit the
226 iteration with the latest values of λ and κ .

227

228 The iterative process in Figure 2 converges to a unique solution, typically within 1-2 iterations.
229 The number of sieves used in the experimental data affects the convergence rate, and the more
230 sieves lead to a faster convergence.

231

232 **PARAMETRIC STUDY AND VALIDATION OF MODEL**

233 In this section, we focus on the influences of model parameters on the shape of PSD and the
234 relationship between the model parameters and classification systems commonly used in
235 geotechnical engineering, such as the coefficient of uniformity C_u and the coefficient of
236 curvature C_c . Besides, the proposed PSD model is verified and compared with other three PSD
237 models (GGSM, GMM, FUM) based on a database of 154 continuous PSD curves (with 127
238 PSD curves broken from initial uniformly graded or non-uniformly graded samples and 27 PSD
239 curves mixed by different group sizes, see the details in section 4 and section 5, respectively).

240

241 The most frequent particle size can directly be obtained by a particle size probability density
242 function plotted in a $\log(d)$ scale (Fredlund et al. 2000). The differentiation of the proposed PSD
243 model in a logarithm form is given by:

$$p(d) = \frac{dP(d)}{d \log(d)} = \frac{\ln(10)\kappa d_{\max}}{\lambda^\kappa} \times \frac{d^\kappa}{(d_{\max} - d)^{\kappa+1}} \times e^{-\left[\frac{d}{\lambda(d_{\max} - d)}\right]^\kappa} \quad (10)$$

245 There are three main types of continuous PSD curves in $P(d)$ - $\log(d)$ space: hyperbolic (Type 1),
 246 S shaped (Type 2), and nearly linear (Type 3) (Zhu et.al. 2015). In order to verify the
 247 performance of the proposed model, we fix d_{\max} at 50mm, and change the values of parameter λ
 248 and κ . The results are shown in Figure 3 and Figure 4.

249
 250 As shown in Figure 3(b), the PSD of Type 1 is a hyperbolic shaped curve in the $P(d)$ - $\log(d)$
 251 space, and the PDF first increases and then decreases with increasing particle size. Type 2 in
 252 Figure 3(c) is an S shaped curve in the $P(d)$ - $\log(d)$ space. The value of $p(d)$ shares the similar
 253 tendency with that of Type 1: first increases and then decreases with increasing particle size.
 254 Both of Type 1 and Type 2 PSD are unimodal distribution. However, a soil with Type 1 PSD has
 255 much more larger particles than Type 2 PSD. PSD of Type 3 as shown in Figure 3(a) is a nearly
 256 linear shaped curve in the $P(d)$ - $\log(d)$ space, and the logarithmic density function increases with
 257 increasing particle size, which means a larger particle size has a larger mass percentage. General
 258 speaking, a soil with Type 3 PSD has the largest amount of large particles.

259
 260 Figure 3 shows the influence of λ on PSD. For a constant κ (0.8) in Figure 3(b), the shape of the
 261 PSD curves are hyperbolic and of Type 1. As λ increases, the PSD becomes steeper. Figure 3(c)
 262 shows a plot of PSD with a constant κ (1.5) and varying λ . Particle sizes become smaller with an
 263 decreasing λ , but the shape of the PSD curves remains almost unchanged (Type 2). For a constant
 264 κ at 0.2, the PSD curves tend to be more linear (Type3, Figure 3(a)). In general, λ does not affect
 265 the shape of the PSD curves much if the value of κ is fixed, but it affects the characteristic
 266 particle sizes, for example d_{10} or d_{50} .

267
 268 Figure 4 shows the influence of κ on PSD. In this figure, for a constant λ , the shape of PSD
 269 changes with parameter κ and all the PSD curves intersect at one point ($d_{63.2}$, 0.632). For
 270 example, for $\kappa=0.2$, the PSD curves are more or less in a linear shape (Type 3, also see Figure 3
 271 (c)), irrespective of λ . As κ increases and λ is kept constant value (Figures 4(a)-4(c)), the shape
 272 of the PSD curves changes from a linear shape (Type 3) to a hyperbolic one (Type 1) and then to
 273 an S shaped (Type 2).

274

275 Figure 5 shows the influence of κ on logarithmic PDF. Again, the PSD curve type will change
276 from Type 3 to Type 1 and then Type 2 with the increasing κ for a fixed λ . According to Figure 5,
277 the most frequent particle size (the size corresponding to the peak value of PDF) will decrease
278 with increasing κ .

279

280 In summary, the proposed PSD model is able to describe continuous PSD curves of the three
281 main types. Moreover, the shape of a PSD curve is mainly affected by parameter κ , with
282 parameter λ affecting characteristic particle diameters.

283

284 Parameters such as the coefficient of uniformity C_u and the coefficient of curvature C_c are
285 commonly used as basic properties of soil in engineering field. Parameter λ has a theoretical
286 solution as shown by Equation (7), and it is an index similar with C_u . The relationship between
287 parameter κ and the coefficient of uniformity C_u , the coefficient of curvature C_c were
288 investigated based on 154 PSD curves (see details in section 4 and section 5).

289

290 Figure 6 and Figure 7 show the correlation between parameter κ and C_c or C_u . Both C_c and C_u
291 decrease with increasing κ and show an asymptote around $\kappa=0.35$. The relationship between κ
292 and C_c or C_u can be expressed as power functions as shown in Figures 6-7. These relationships
293 seem to be independent of the tested material or the testing method, as the experimental data
294 listed in Table 1 include different soils in different tests. The correlations shown in Figure 6-7
295 indicate that parameter κ can be estimated with confidence from commonly used soil grading
296 parameters. For example, as the solid square points shown in Figures 6-7, parameter $\kappa=0.927$,
297 0.372, 3.00 when $C_u=5$, $C_c=1$ and $C_c=3$, respectively, which means the parameter κ should be
298 within the range of 0.372 to 0.927 if the soil sample is expected to be well graded based on the
299 standard for engineering classification of soils in China (GB/T50145-2007).

300

301 To verify the proposed PSD model, fifty-three (53) sets of granular materials with 154 PSD
302 curves are used to evaluate the applicability of proposed model. Those PSD curves are all non-
303 uniformly and continuous graded, some of them break from uniformly graded samples (see the
304 details in section 4) and others are an arbitrary mixture of particles from different group sizes

305 (see the details in section 5). Moreover, other three PSD models (GGSM, GMM, and FUM) are
306 also used for comparison. The results are shown in Figure 8.

307
308 Figure 8 shows the variation of the correlation coefficient R^2 versus the particle diameter $d_{63.2}$.
309 The reason that we choose $d_{63.2}$ is that $d_{63.2}$ is an important particle size and determines the value
310 of λ in this study. The values of $d_{63.2}$ are obtained by setting $P(d_{63.2})=0.632$ to Equation (6). An
311 R^2 value closer to 1 indicates a better fitting. As shown in Figure 8, the prediction of the
312 proposed model is relatively good across different values of $d_{63.2}$. The overall performance of the
313 GGSM model is better than the GMM model, although some values of R^2 of the GMM are larger
314 than those of GGSM's in certain cases. The model proposed in this paper and FUM are superior
315 to the previous two models. In general, the model proposed in this paper is able to capture a wide
316 variety of PSDs from the literature and it performs better than the FUM model while having less
317 fitting parameters and simple mathematical form.

318 319 **EVOLVING PARTICLE SIZE DISTRIBUTIONS DUE TO BREAKAGE**

320 In this section, twenty-six (26) sets of granular materials with 127 PSD curves are used to
321 evaluate the applicability of the proposed model involving particle breakage. The selected
322 experimental data covers different material properties and loading types and most of the curves
323 are obtained from tests designed to induce particle crushing tests (Bard 1993; Hagerty et al.
324 1993; Luzzani and Coop 2002; Coop et al. 2004; Russell and Khalili 2004; Okada et al. 2004;
325 Mayoraz et al. 2006; Guimares et al. 2007; Kikumoto et al. 2010; Xiao et al. 2014, 2016; Zhang
326 et al. 2017). Some typical detailed fitting results are shown in Table 1. The fitting of
327 experimental data in Table 1 was done individually for each PSD curve, which allows us to
328 examine the general capacity of the proposed model in predicting evolving PSD curves.

329
330 Table 1 shows the fitting results of the experimental data of the four PSD models. The
331 performances of different PSD models can be evaluated by the correlation coefficient R^2 . In
332 Table 1, there is a consistent and monotonic evolution of the 2 fitting parameters (λ and κ) of the
333 proposed model in most cases, except for the data from Coop et al. (2004) at very large strains.
334 The reason for this inconsistent and non-monotonic evolution of 2 parameters is either an

335 experimental error or particle aggregation. The test results in [Coop et al. \(2004\)](#) showed that the
 336 number of fine particles first increased with increasing strain and then dropped at very high
 337 strains, which is not possible unless particle aggregation occurs at large strains. The proposed
 338 model does not consider particle aggregation. It is noted that the performance of FUM model is
 339 only verified by those PSD data with more than eight sieving points in Figure 8 and Table 1,
 340 because the fitting results may be unreliable when the sieving points are too few to fit for the
 341 four fitting parameters.

342
 343 According to the data in Table 1, the GGSM model and GMM model have a relatively good
 344 performance for describing PSD curves for specimens at relatively low stresses or strains (with
 345 less particle breakage). However, at large stress or strain, the predictions of the proposed model
 346 and FUM model become significantly better than the GGSM model and GMM model, implying
 347 that the proposed model captures the particle breakage better than the GGSM and the GMM
 348 models.

349
 350 As mentioned above, the evolution of PSD curves during particle breakage exhibits certain
 351 trends, which are easily identifiable for initially uniformly graded samples. Ideally these trends
 352 should be captured in the PSD model. Figure 9 shows the evolution of the two model parameters
 353 (λ and κ) with stresses or strains for a range of tests and materials. Both parameters follow clear
 354 trends during breakage, decreasing with increasing stresses or strains (or increasing extent of
 355 breakage) and approaching stationary values at high degrees of breakage. The following equation
 356 provides a relatively good prediction of the evolution of the two parameters (λ and κ):

$$357 \quad \lambda = a_\lambda + b_\lambda e^{c_\lambda \sigma(\gamma, p)}, \quad \kappa = a_\kappa + b_\kappa e^{c_\kappa \sigma(\gamma, p)} \quad (11)$$

358 where a , b , c are fitting parameters, $\sigma(\gamma, p)$ is stress (strain) in the test. With Equation (11), only
 359 two sets of parameters (a , b , c) or total six parameters are needed to predict the PSD curve at an
 360 arbitrary degree of breakage, which is an important advantage of the proposed model.

361

362 ASSESSING INTERNAL STABILITY OF WIDELY GRADED GRANULAR SOILS

363 In addition to particle breakage, the PSD model proposed in this paper can also be applied to
 364 assess internal stability of granular filters. One of the most commonly used geometric criteria is
 365 the criterion by Kenney and Lau (1985 and 1986). A geometric index ratio of H/F was proposed
 366 and applied in the analysis of internal stability of granular soils. A granular sample would be
 367 considered as unstable if

$$368 \quad (H/F)_{\min} < 1 \quad (12)$$

369 where H is the mass fraction of particles with size from d to $4d$, F is the mass fraction of
 370 particles with size finer than d as shown in Figure 10. For a widely graded and uniformly graded
 371 sample, the search for the minimum value of H/F will end at $F=20\%$ and $F=30\%$ respectively.
 372

373 For a widely graded granular soil (with minimum particle size 0.063mm), the whole PSD curve
 374 can be represented by the proposed PSD model as shown in Equation (6). Substituting Equation
 375 (6) into Equation (12) leads to:

$$376 \quad \left\{ \frac{e^{-\left(\frac{d}{\lambda(d_{\max}-d)}\right)^{\kappa}} - e^{-\left(\frac{4d}{\lambda(d_{\max}-4d)}\right)^{\kappa}}}{1 - e^{-\left(\frac{d}{\lambda(d_{\max}-d)}\right)^{\kappa}}} \right\}_{\min} < 1, \quad 0.063 < d \leq \frac{d_{\max}}{4} \quad (13)$$

377 Equation (13) means that for a given particle size d (from 0.063 to $d_{\max}/4$), the value of H/F is
 378 always less than 1. It is a linear programming problem to some extent. The maximum value of
 379 $d_{\max} \leq 100\text{mm}$ for most granular soils. Letting $d_{\max}/d=y$, the range of y values should be from 4 to
 380 $100/0.063(\approx 1600)$. Equation (13) can then be expressed as

$$381 \quad \begin{cases} \left(2e^{-\left(\frac{1}{\lambda(y-1)}\right)^{\kappa}} - e^{-\left(\frac{1}{\lambda\left(\frac{1}{4}(y-1)}\right)^{\kappa}} - 1 \right) /_{4 \leq y \leq 1600}} < 0 \\ \lambda > 0 \\ \kappa > 0 \end{cases} \quad (14)$$

382 Letting $f(y) = 2e^{-\left(\frac{1}{\lambda(y-1)}\right)^\kappa} - e^{-\left(\frac{1}{\lambda\left(\frac{1}{4}(y-1)\right)}\right)^\kappa} - 1$, we can plot $f(y)=0$ in λ - κ space for any $4 \leq y \leq 1600$, as
 383 shown in Figure 11.

384

385 Figure 11 shows some typical curves of $f(y)=0$ in λ - κ space for given y . In general, the curve of
 386 $f(y)=0$ tends to be flat with increasing y . In the case of $y=4$, the relationship between λ and κ is be
 387 plotted as curve 1, while, in the case of $y=1600$, the relationship between λ and κ is plotted as
 388 curve 8. Since for any y ($4 \leq y \leq 1600$), $f(y)$ needs to satisfy $f(y) < 0$, that is to say, the range of λ and
 389 κ needs to below all the curves of $f(y)=0$ for any y ($4 \leq y \leq 1600$). In other words, if the granular
 390 sample would be considered unstable, the range of λ and κ should fall within the area below
 391 curves AB and BC (Area 1, the intersection of all the range of λ and κ for any y) as shown in
 392 Figure 11. Point B is the intersection of curve 1 and curve 8.

393

394 The same method for determining the range of λ and κ for the consideration of stable of granular
 395 soils since the criterion should be rewritten as:

$$396 \quad (H/F)_{\min} \geq 1 \quad (15)$$

397 Similar conclusion can be obtained that the granular sample would be considered stable if the
 398 range of λ and κ falls in the area above curves DB and BE (Area 2). It is worth noting that this
 399 area is not, but very close to, the real area because the intersections of all the curves of λ and κ
 400 for any given y are close to, but not exactly at point B. Here, for simplicity, we use point B to
 401 distinguish the area of λ and κ when assessing the internal stability for soil samples.

402

403 Data of internal stability tests on 27 widely graded granular soils from the literature ([Kenney and](#)
 404 [Lau 1985](#); [Aberg 1993](#); [Indraratna et al. 2015](#); [Skempton and Brogan 1994](#)) are collected and
 405 used for verifying the stable and unstable areas proposed in the λ - κ space. PSD parameters λ and
 406 κ are first obtained using fitting process as shown in Figure 2, and their values are then plotted in
 407 the λ - κ space. The results are shown in Figure 12.

408

409 Figure 12 shows that more than 50% (10/18) of the stable grading fall into the proposed stable
 410 area, 7 stable grading fall into area 4, while, and only 1 stable grading falls into the unstable area.

411 Unstable gradings tested in the laboratory fall into stable area, unstable area and other two areas
412 with the same proportion (3/9). For areas 3 and 4, Equation (12) and Equation (15) are not
413 always satisfied for any y . If both Equation (12) (or Equation (15)) and $F \leq 20\%$ are met, the
414 granular soil sample can be regarded as unstable (or stable). That is to say, for the PSD
415 parameters λ and κ falling into area 3 and area 4, the internal stability of the granular soil cannot
416 be determined and needs further assessment.

417
418 The stable area and unstable area proposed in this paper are based on Kenney and Lau's
419 criterion. It is a more straightforward and simpler way for assessing internal stability of widely
420 graded granular soils, compared against other methods in the literature. As shown in Figure 12,
421 the stable and unstable area defined in the λ - κ space are in relatively good agreement with
422 experimental results.

423

424 CONCLUSIONS

425 A simple particle size distribution model for granular materials is proposed in this paper. The
426 model contains two parameters, one parameter (λ) representing a characteristics particle
427 diameter, and the other parameter κ closely correlated to the coefficient of uniformity (C_u) or the
428 coefficient of curvature (C_c). Parameter κ mainly affects the shape of the PSD curve, while
429 parameter λ affects characteristic particle sizes of the soil sample.

430

431 The proposed PSD model can capture the main types of continuous PSD curves. Its performance
432 is compared against the Gates-Gaudin-Schuhmann model, Gaudin-Mellog model and Fredlund
433 unimodal model by analysing 53 soil specimens with 154 PSD curves. It is shown that the
434 proposed PSD model performs better than the Gates-Gaudin-Schuhmann model and the Gaudin-
435 Mellog model, particularly for PSD curves obtained at high degrees of particle breakage. The
436 proposed two-parameter PSD model displays a similar performance to the four-parameter
437 Fredlund unimodal model. It is shown that the two parameters in the proposed model follow
438 clear trends identifiable during particle breakage of initially uniformly graded soil samples.
439 Equations are proposed for these trends, with which the evolution of PSD curves during particle
440 breakage of one soil sample can be predicted with two sets of model parameters.

441

442 A continuous particle size distribution model provides a quantitative method for estimating other
443 soil properties and is an important element in studying problems such as particle breakage and
444 assessment of internal stability. An initially non-uniformly graded sample can be treated either as
445 the product of a uniformly graded sample due to particle breakage, or an arbitrary mixture of
446 particles from different group sizes (Zhang et al. 2015). For initially non-uniformly graded
447 samples, the situation can be more complex. The proposed model can be extended to capture
448 more complex PSDs (e.g. bimodal distributions representative of gap-graded soils) through
449 superposition of two or more unimodal PSDs.

450

451

452 ACKNOWLEDGEMENTS

453 This research was partly supported by the National Basic Research Program of China (no.
454 2014CB047001). The first author would like to acknowledge the support of the China
455 Scholarship Council.

456

457

458 REFERENCES

459 Åberg, B. 1993. Washout of grains from filtered sand and gravel materials. *Journal of*
460 *Geotechnical Engineering*, 119(1), 36-53.

461 Altuhafi, F. N., and Coop, M. R. 2011. Changes to particle characteristics associated with the
462 compression of sands. *Géotechnique*, 61(6), 459–471.

463 Bard E., 1993. Comportement des matériaux granulaires secs et à liant hydrocarboné, thèse de
464 Doctorat, École Centrale de Paris.

465 Bayat, H., Rastgo, M., Zadeh, M. M., and Vereecken, H. 2015. Particle size distribution models,
466 their characteristics and fitting capability. *Journal of Hydrology*, 529, 872-889.

467 Coop, M. R., Sorensen, K. K., Freitas, T. B., and Georgoutsos, G. 2004. Particle breakage during
468 shearing of a carbonate sand. *Géotechnique*, 54(3), 157-164.

469 El Mohtar, C. S., Yoon, J., and El-Khattab, M. 2015. Experimental study on penetration of
470 bentonite grout through granular soils. *Canadian Geotechnical Journal*, 52(11), 1850-1860.

471 Einav, I. 2007. Breakage mechanics—part I: theory. *Journal of the Mechanics and Physics of*
472 *Solids*, 55(6), 1274-1297.

- 473 Fredlund, M. D., Fredlund, D. G., and Wilson, G. W. 2000. An equation to represent grain-size
474 distribution. *Canadian Geotechnical Journal*, 37(4), 817-827.
- 475 Fredlund, M. D., Wilson, G. W., and Fredlund, D. G. 2002. Use of the grain-size distribution for
476 estimation of the soil-water characteristic curve. *Canadian Geotechnical Journal*, 39(5),
477 1103-1117.
- 478 Fuller, W. B., Thompson, S. E., 1906. The laws of proportioning concrete. Transactions of the
479 American Society of Civil Engineers, 57(2): 67-143.
- 480 Guimaraes, M. S., Valdes, J. R., Palomino, A. M., and Santamarina, J. C. 2007. Aggregate
481 production: fines generation during rock crushing. *International Journal of Mineral*
482 *Processing*, 81(4), 237-247.
- 483 Gallage, C. P. K., and Uchimura, T. 2010. Effects of dry density and grain size distribution on
484 soil-water characteristic curves of sandy soils. *Soils and Foundations*, 50(1), 161-172.
- 485 Hagerty, M. M., Hite, D. R., Ullrich, C. R., and Hagerty, D. J. 1993. One-dimensional high-
486 pressure compression of granular media. *Journal of Geotechnical Engineering*, 119(1), 1-18.
- 487 Hardin, B. O. 1985. Crushing of soil particles. *Journal of Geotechnical Engineering*, 111(10),
488 1177-1192.
- 489 Harris, C. C. 1968. The application of size distribution equations to multi-event comminution
490 processes. *Trans. AIME*, 241, 343-358.
- 491 Hwang, S. I., Lee, K. P., Lee, D. S., and Powers, S. E. 2002. Models for estimating soil particle-
492 size distributions. *Soil Science Society of America Journal*, 66(4), 1143-1150.
- 493 Hyodo, M., Wu, Y., Aramaki, N., and Nakata, Y. 2017. Undrained monotonic and cyclic shear
494 response and particle crushing of silica sand at low and high pressures. *Canadian*
495 *Geotechnical Journal*, 54(2), 207-218.
- 496 Indraratna, B., Raut, A. K., and Khabbaz, H. 2007. Constriction-based retention criterion for
497 granular filter design. *Journal of Geotechnical and Geoenvironmental Engineering*, 133(3),
498 266-276.
- 499 Indraratna, B., Israr, J., and Rujikiatkamjorn, C. 2015. Geometrical method for evaluating the
500 internal instability of granular filters based on constriction size distribution. *Journal of*
501 *Geotechnical and Geoenvironmental Engineering*, 141(10), 04015045.
- 502 Karol, R. H. 1990. *Chemical grouting*. Marcel Dekker.
- 503 Kenney, T. C., and Lau, D. 1985. Internal stability of granular filters. *Canadian Geotechnical*
504 *Journal*, 22(2), 215-225.
- 505 Kenney, T. C., and Lau, D. 1986. Internal stability of granular filters: Reply. *Canadian*
506 *Geotechnical Journal*, 23(3), 420-423.

- 507 Kikumoto, M., Muir Wood, D. and Russell, A. 2010. Particle crushing and deformation
508 behaviour. *Soils and Foundations*, 50(4), 547-563.
- 509 Lee, K. L., and Farhoomand, I. 1967. Compressibility and crushing of granular soil in
510 anisotropic triaxial compression. *Canadian Geotechnical Journal*, 4(1), 68-86.
- 511 Luo, H., Cooper, W. L., and Lu, H. 2014. Effects of particle size and moisture on the
512 compressive behavior of dense Eglin sand under confinement at high strain rates.
513 *International Journal of Impact Engineering*, 65, 40-55.
- 514 Luzzani, L., and Coop, M. R. 2002. On the relationship between particle breakage and the
515 critical state of sands. *Soils and Foundations*, 42(2), 71-82.
- 516 Marsal, R. J. 1967. Large-scale testing of rockfill materials. *Journal of the Soil Mechanics and*
517 *Foundations Division*, 93(2), 27-43.
- 518 MATLAB and Statistics Toolbox Release R2016b, The MathWorks, Inc., Natick, Massachusetts,
519 United States.
- 520 Mayoraz, F., Vulliet, L., and Laloui, L. 2006. Attrition and particle breakage under monotonic
521 and cyclic loading. *Comptes Rendus Mécanique*, 334(1), 1-7.
- 522 McDowell, G. R., Bolton, M. D., and Robertson, D. 1996. The fractal crushing of granular
523 materials. *Journal of the Mechanics and Physics of Solids*, 44(12), 2079-2101.
- 524 Merkus, H. G. 2009. Particle size measurements: fundamentals, practice, quality. Springer
525 Science & Business Media.
- 526 Miao, G., and Airey, D. 2013. Breakage and ultimate states for a carbonate sand. *Géotechnique*,
527 63(14), 1221-1229.
- 528 Moraci, N., Mandaglio, M. C., and Ielo, D. 2014. Analysis of the internal stability of granular
529 soils using different methods. *Canadian Geotechnical Journal*, 51(9), 1063-1072.
- 530 Moraci, N., Mandaglio, M. C., and Ielo, D. 2015. Reply to the discussion by Ni et al. on
531 "Analysis of the internal stability of granular soils using different methods". *Canadian*
532 *Geotechnical Journal*, 52(3), 385-391.
- 533 Muir Wood, D., and Maeda, K. 2008. Changing grading of soil: effect on critical states. *Acta*
534 *Geotechnica*, 3(1), 3-14.
- 535 Nakata, Y., Hyodo, M., Hyde, A. F., Kato, Y., and Murata, H. 2001. Microscopic particle
536 crushing of sand subjected to high pressure one-dimensional compression. *Soils and*
537 *Foundations*, 41(1), 69-82.
- 538 Okada, Y., Sassa, K., and Fukuoka, H. 2004. Excess pore pressure and grain crushing of sands by
539 means of undrained and naturally drained ring-shear tests. *Engineering Geology*, 75(3), 325-
540 343.

- 541 Ouyang, M., and Takahashi, A. 2016a. Influence of initial fines content on fabric of soils
542 subjected to internal erosion. *Canadian Geotechnical Journal*, 53(2), 299-313.
- 543 Ouyang, M., and Takahashi, A. 2016b. Reply to the discussion by Ahmad Alsakran et al. on
544 “Influence of initial fines content on fabric of soils subjected to internal erosion”. *Canadian*
545 *Geotechnical Journal*, 53(8), 1360-1361.
- 546 Russell, A. R., and Khalili, N. 2004. A bounding surface plasticity model for sands exhibiting
547 particle crushing. *Canadian Geotechnical Journal*, 41(6), 1179-1192.
- 548 Sammis, C., King, G., and Biegel, R. 1987. The kinematics of gouge deformation. *Pure and*
549 *Applied Geophysics*, 125(5), 777-812.
- 550 Sanvitale, N., and Bowman, E.T. 2017. Visualization of dominant stress-transfer mechanisms in
551 experimental debris flows of different particle-size distribution. *Canadian Geotechnical*
552 *Journal*, 54(2): 258-269.
- 553 Schuhmann Jr, R. 1940. Principles of Comminution, I-Size Distribution and Surface
554 Calculations. American Institute of Mining, Metallurgical, and Petroleum Engineers,
555 Englewood, CO, AIME Technical Publication, (1189).
- 556 Skempton, A. W., and Brogan, J. M. 1994. Experiments on piping in sandy gravels.
557 *Geotechnique*, 44(3), 449-460.
- 558 Standard GB/T50145 2007. Standard for engineering classification of soil. (in Chinese)
- 559 Talbot, A. N., Richart, F. E., 1923. The strength of concrete-its relation to the cement, aggregates
560 and water. Illinois Univ Eng Exp Sta Bulletin, 137: 1-118.
- 561 Tong, C. X., Zhang S., Li X., and Sheng D. 2015. Evolution of geotechnical materials based on
562 Markov chain considering particle crushing. *Chinese Journal of Geotechnical Engineering*,
563 37(5), 870-877 (in Chinese).
- 564 Vipulanandan, C., and Ozgurel, H. G. 2009. Simplified relationships for particle-size distribution
565 and permeation groutability limits for soils. *Journal of Geotechnical and Geoenvironmental*
566 *Engineering*, 135(9), 1190-1197.
- 567 Wan, C. F., and Fell, R. 2008. Assessing the potential of internal instability and suffusion in
568 embankment dams and their foundations. *Journal of Geotechnical and Geoenvironmental*
569 *Engineering*, 134(3), 401-407.
- 570 Xiao, Y., Liu, H., Chen, Y., and Jiang, J. 2014. Strength and deformation of rockfill material
571 based on large-scale triaxial compression tests. II: influence of particle breakage. *Journal of*
572 *Geotechnical and Geoenvironmental Engineering*, 140(12), 04014071.
- 573 Xiao, Y., Liu, H., Xiao, P., and Xiang, J. 2016. Fractal crushing of carbonate sands under impact
574 loading. *Géotechnique Letters*, 6(3), 199-204.

- 575 Zhang, J., Li, M., Liu, Z., and Zhou, N. 2017. Fractal characteristics of crushed particles of coal
576 gangue under compaction. *Powder Technology*, 305, 12-18.
- 577 Zhang, S., Tong, C. X., Li, X., and Sheng, D. 2015. A new method for studying the evolution of
578 particle breakage. *Géotechnique*, 65(11), 911-922.
- 579 Zhang, X., and Baudet, B. A. 2013. Particle breakage in gap-graded soil. *Géotechnique Letters*,
580 3(2), 72-77.
- 581 Zheng, W., and Tannant, D. 2016. Frac sand crushing characteristics and morphology changes
582 under high compressive stress and implications for sand pack permeability. *Canadian*
583 *Geotechnical Journal*, 53(9), 1412-1423.
- 584 Zhou, Z. Q., Ranjith, P. J., and Li, S. C. 2016. Optimal model for particle size distribution of
585 granular soil. *Proceedings of the Institution of Civil Engineers - Geotechnical Engineering*,
586 169(1), 73-82.
- 587 Zhu, J. G., Guo, W. L., Wang, Y. L., and Wen, Y. F. 2015. Equation for soil gradation curve and
588 its applicability. *Chinese Journal of Geotechnical Engineering*, 37(10): 1931-1936. (in
589 Chinese)
- 590

591 **List of Figures**

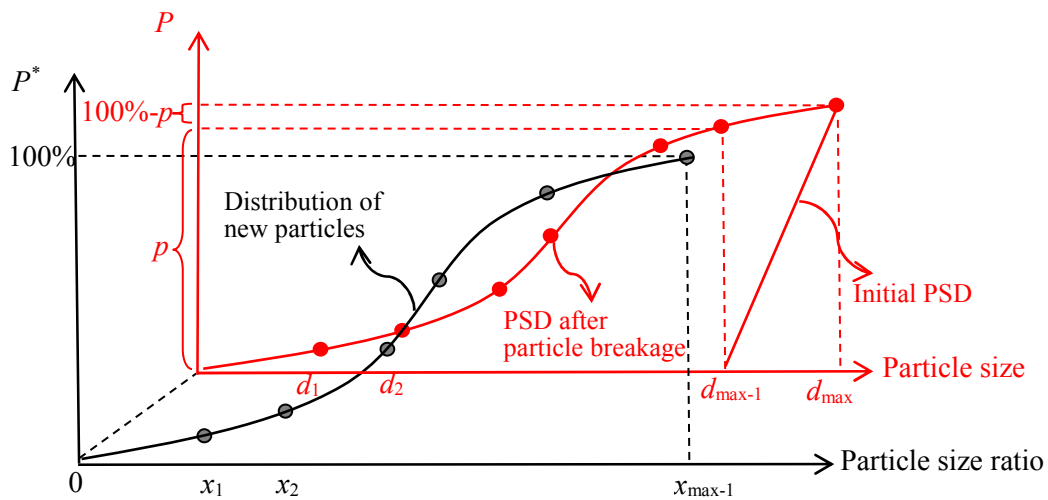
- 592
- 593 Fig. 1. Schematic diagram of PSD of uniformly graded sample after particle breakage
- 594
- 595 Fig. 2. Flow chart for obtaining and assessing parameter λ and κ
- 596
- 597 Fig. 3. Influence of parameter λ on particle size distribution: (a) varying of λ with a fixed $\kappa=0.2$;
- 598 (b) varying of λ with a fixed $\kappa=0.8$; (c) varying of λ with a fixed $\kappa=1.5$.
- 599
- 600 Fig. 4. Influence of parameter κ on particle size distribution: (a) varying of κ with a fixed $\lambda=0.2$;
- 601 (b) varying of κ with a fixed $\lambda=0.8$; (c) varying of κ with a fixed $\lambda=1.5$.
- 602
- 603 Fig. 5. Influence of parameter κ on logarithmic PDF: (a) varying of κ with a fixed $\lambda=0.2$; (b)
- 604 varying of κ with a fixed $\lambda=0.8$; (c) varying of κ with a fixed $\lambda=1.5$.
- 605
- 606 Fig. 6. Correlation between parameter κ and coefficient of non-uniformity C_u
- 607
- 608 Fig. 7. Correlation between parameter κ and coefficient of curvature C_c
- 609
- 610 Fig. 8. Performance of the four PSD models at different particle diameters $d_{63,2}$.
- 611
- 612 Fig. 9. Evolution of model parameters with particle breakage: (a) data from Bard (1993); (b)-(c)
- 613 data from Coop et al. (2004); (d) data from Hagerty et al. (1993); (e) data from Russell and
- 614 Khalili (2004).
- 615
- 616 Fig. 10. Illustration of Kenny and Lau's criterion.
- 617
- 618 Fig. 11. Curves of $f(y)=0$ in λ - κ space
- 619
- 620 Fig. 12. Validation of internal stability of well-graded granular soil
- 621

622 **List of Tables**

623

624 Table 1. Performance of four PSD models for different materials

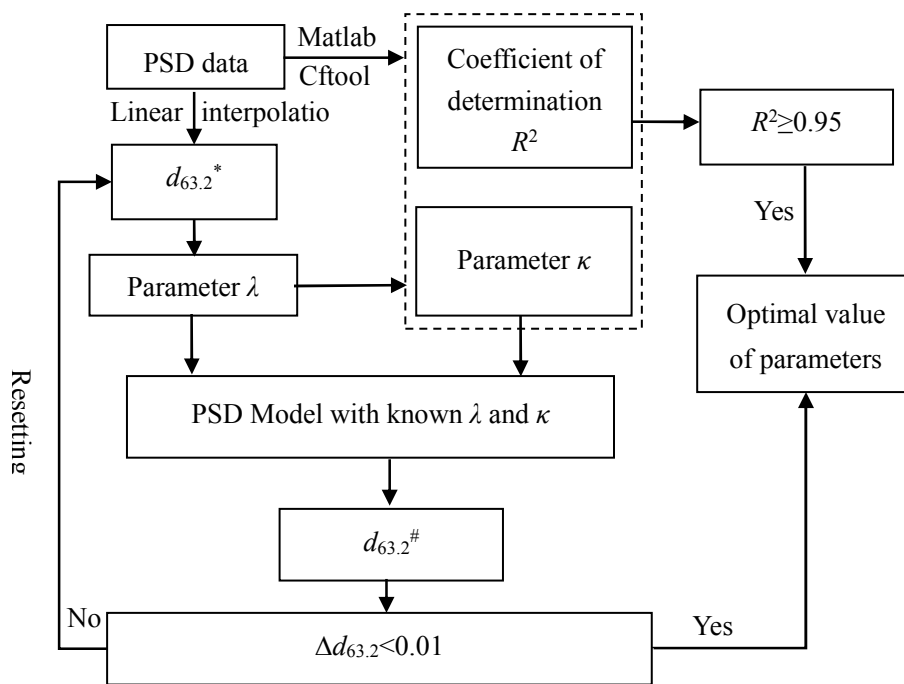
625



$$x_i = d_i / d_{\max-1}$$

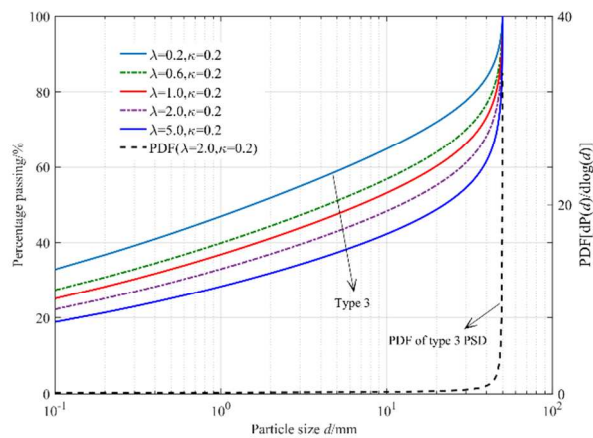
1

2 Fig. 1. Schematic diagram of PSD of uniformly graded sample after particle breakage

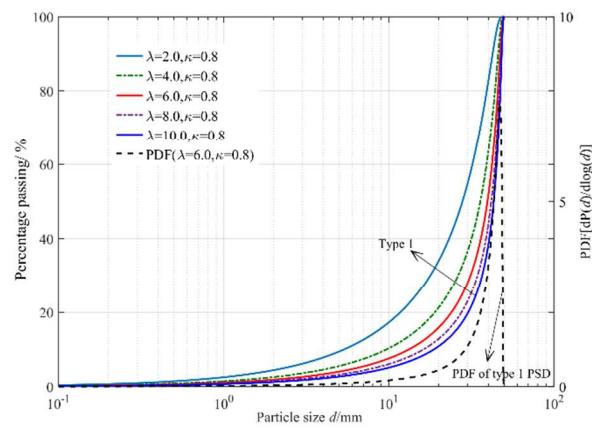


3

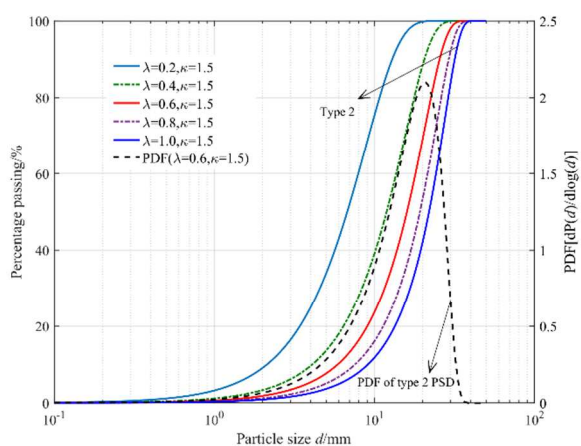
4 Fig. 2. Flow chart for obtaining and assessing parameter λ and κ



(a)

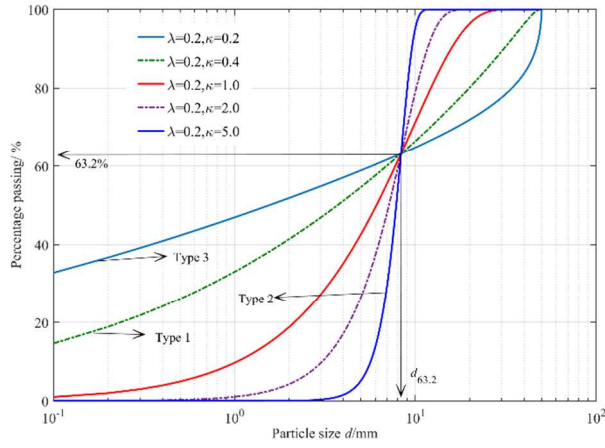


(b)

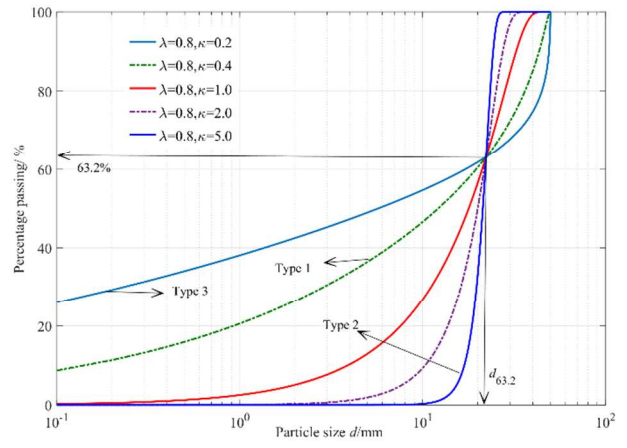


(c)

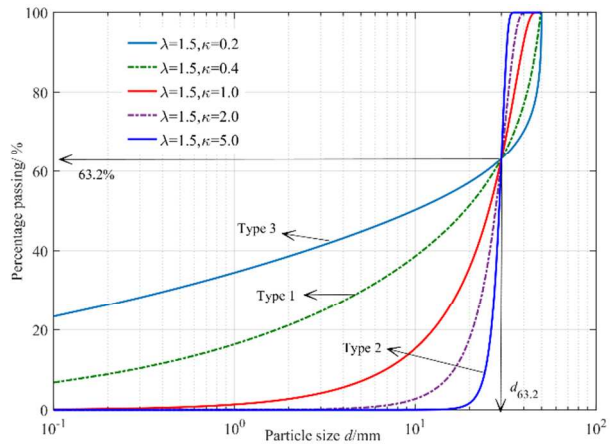
5
6
7
8
9 Fig. 3. Influence of parameter λ on particle size distribution: (a) varying of λ with a fixed $\kappa=0.2$;
10 (b) varying of λ with a fixed $\kappa=0.8$; (c) varying of λ with a fixed $\kappa=1.5$.



(a)



(b)

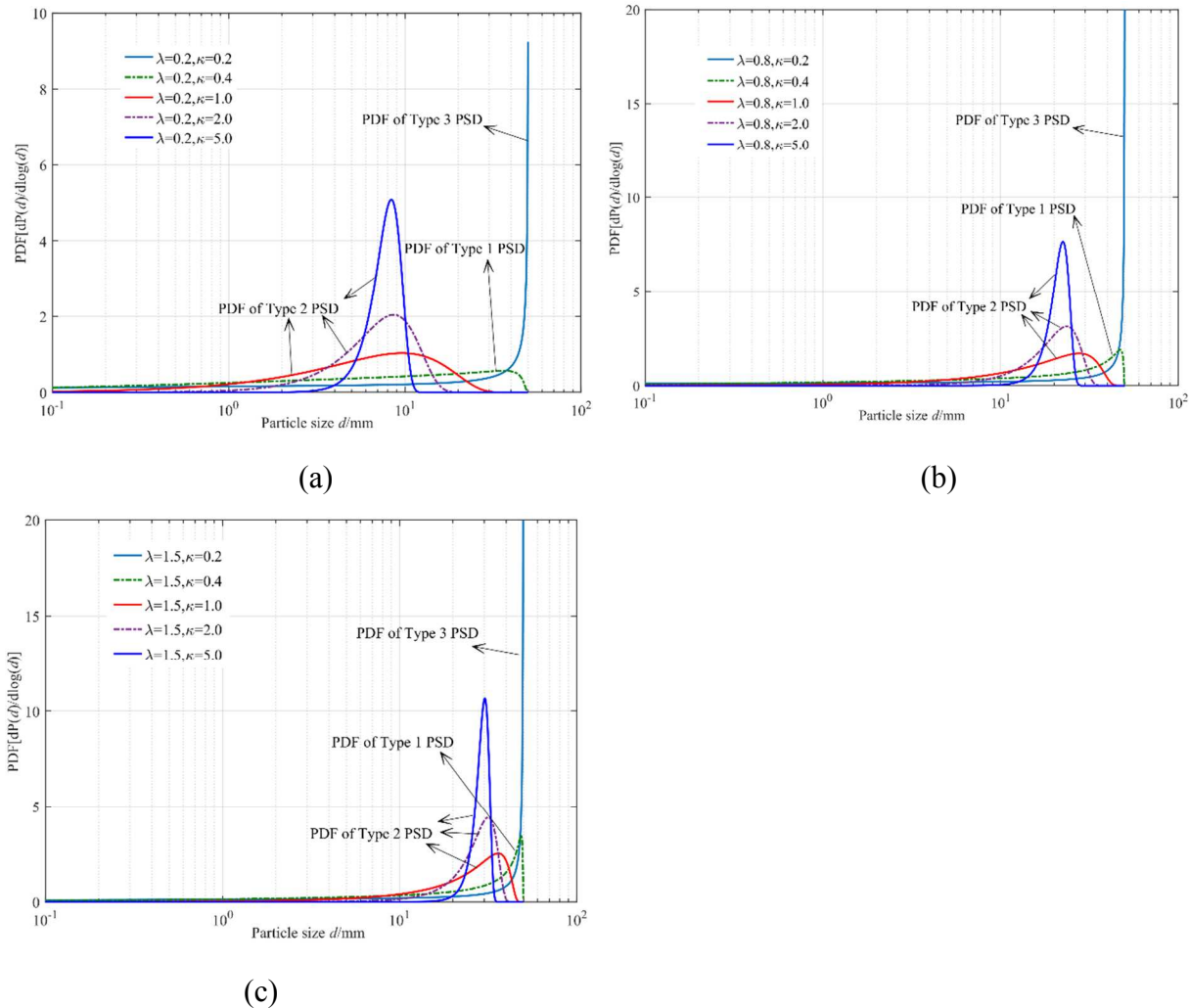


(c)

11
12

13
14

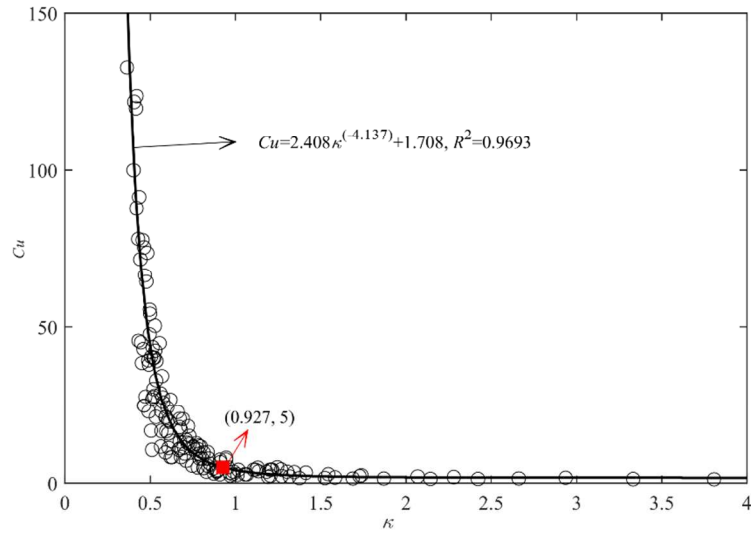
15 Fig. 4. Influence of parameter κ on particle size distribution: (a) varying of κ with a fixed $\lambda=0.2$;
 16 (b) varying of κ with a fixed $\lambda =0.8$; (c) varying of κ with a fixed $\lambda =1.5$.



17
18

19
20

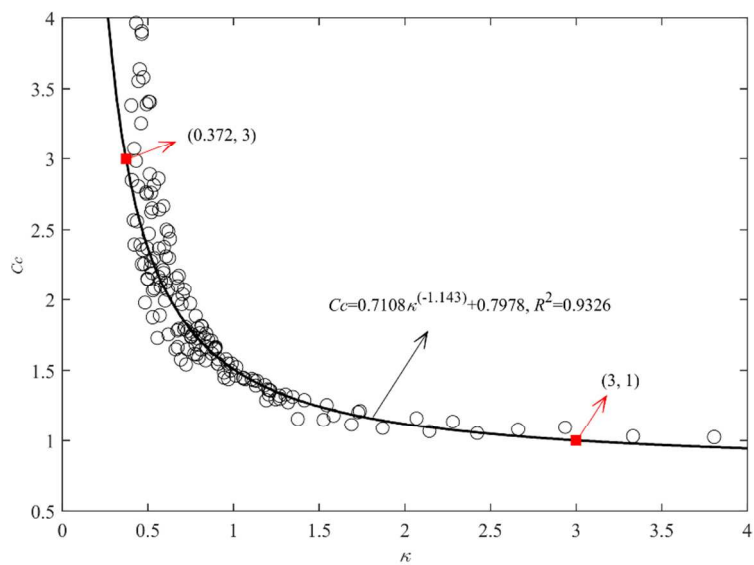
21 Fig. 5. Influence of parameter κ on logarithmic PDF: (a) varying of κ with a fixed $\lambda=0.2$; (b)
22 varying of κ with a fixed $\lambda = 0.8$; (c) varying of κ with a fixed $\lambda = 1.5$.



23

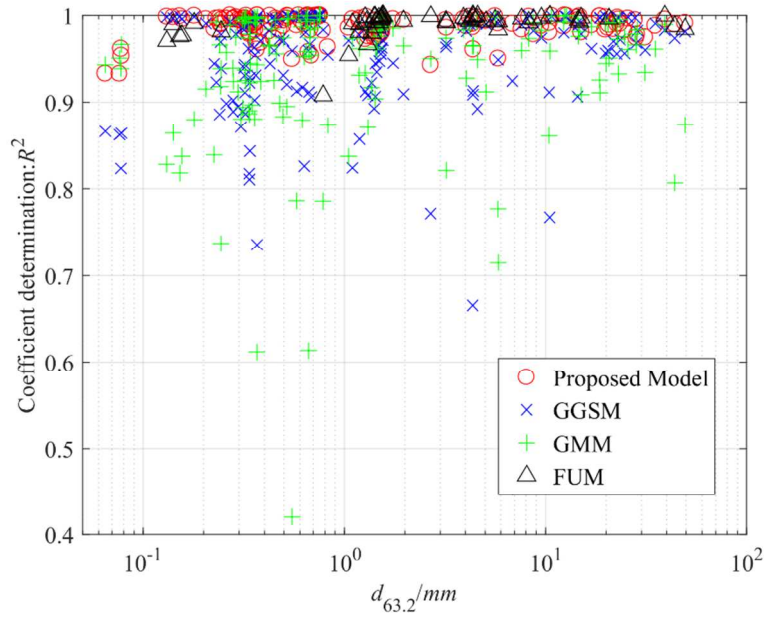
24

Fig. 6. Correlation between parameter κ and coefficient of non-uniformity C_u



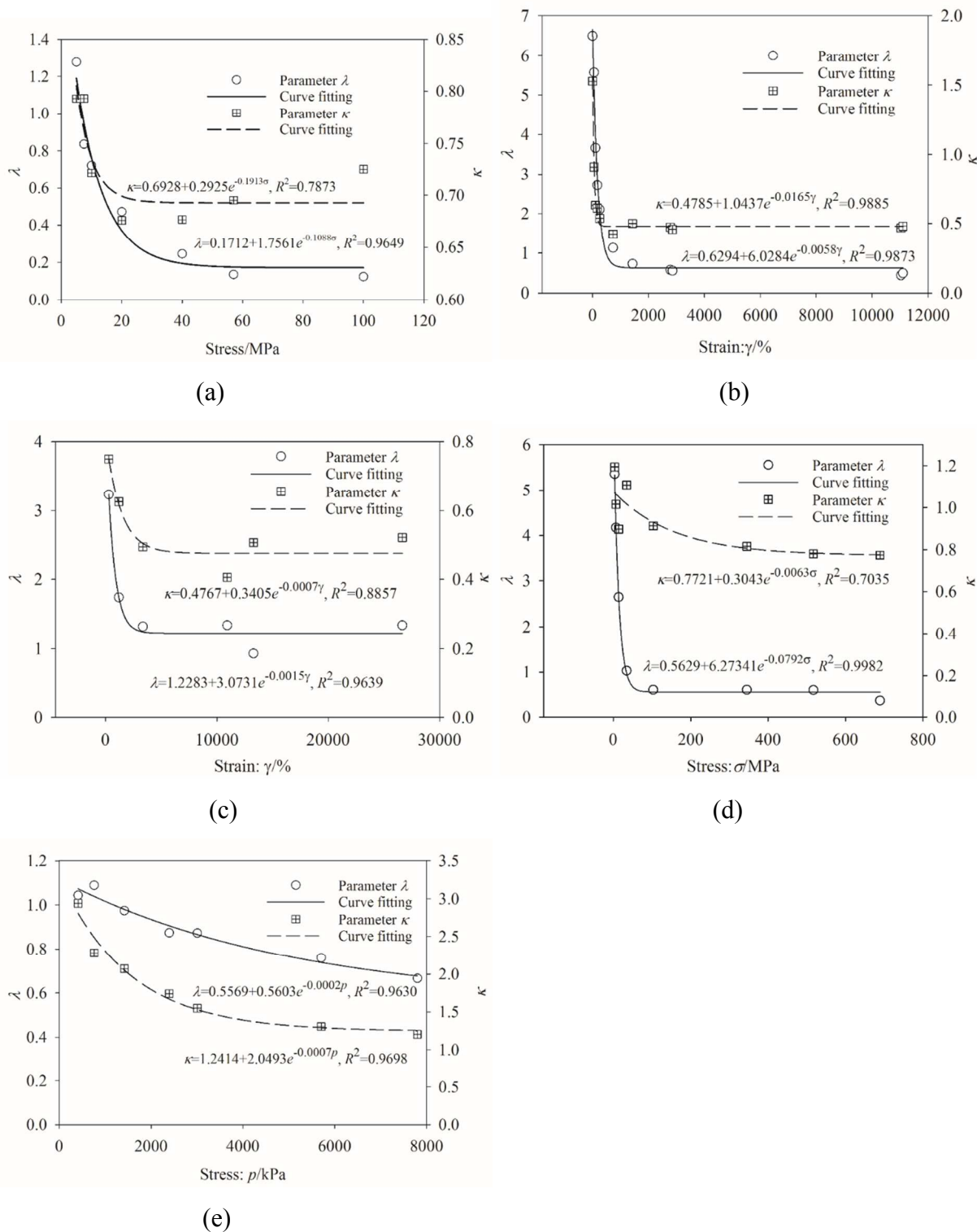
25

26 Fig. 7. Correlation between parameter κ and coefficient of curvature C_c



27

28 Fig. 8. Performance of the four PSD models at different particle diameters $d_{63.2}$.



29

30

31

32

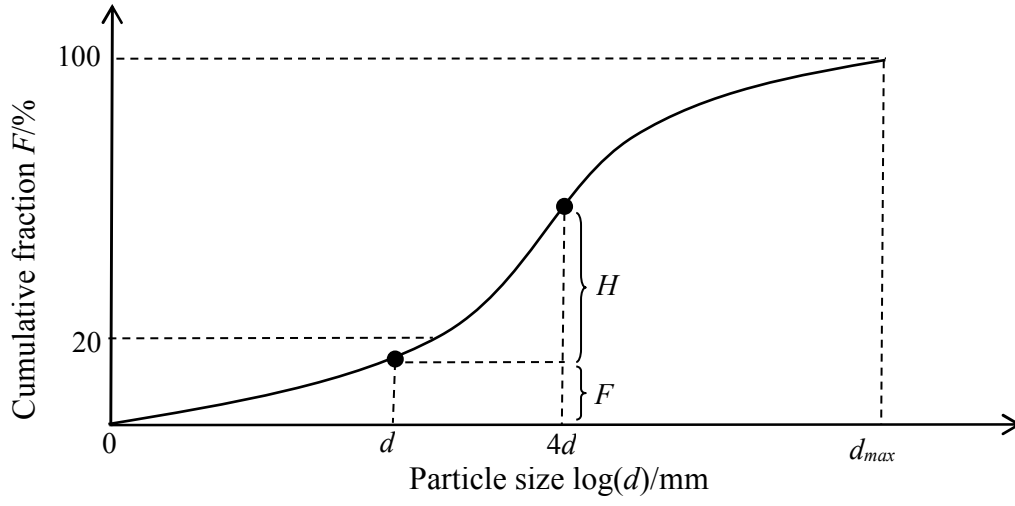
33

34

35 Fig. 9. Evolution of model parameters with particle breakage: (a) data from Bard (1993); (b)-(c)

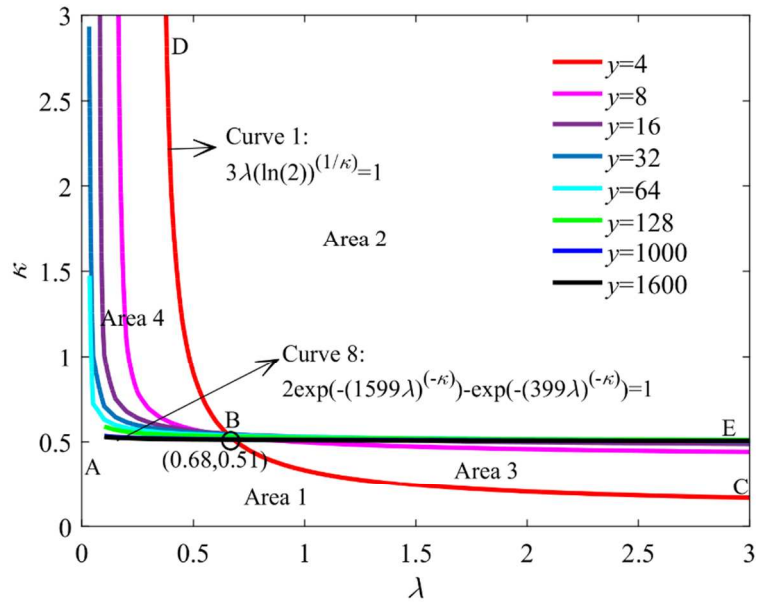
36 data from Coop et al. (2004); (d) data from Hagerty et al. (1993); (e) data from Russell & Khalili

37 (2004).



38

39 Fig. 10. Illustration of Kenny and Lau's criterion.



40

41 Fig. 11. Curves of $f(y)=0$ in λ - κ space

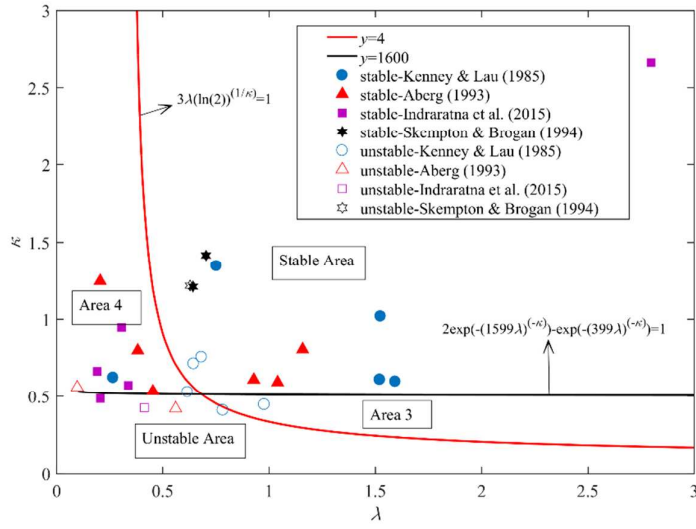


Fig. 12. Validation of internal stability of well-graded granular soil

1 Table 1. Performance of four PSD models for different materials

Reference	Property/Loading	Proposed Model			GGMM	GMM	FUM
		λ	κ	R^2	R^2	R^2	R^2
Coop et al. (2004)	CS/UG/RS/VS1/no shearing	6.498	1.528	0.9997	0.9981	0.9959	0.9908 0.9768 0.9757 0.9702 0.9896 0.9815
	CS/UG/RS/VS1/ $\gamma=52\%$	5.572	0.911	0.9833	0.9545	0.9963	
	CS/UG/RS/VS1/ $\gamma=104\%$	3.664	0.632	0.9935	0.9616	0.9912	
	CS/UG/RS/VS1/ $\gamma=171\%$	2.716	0.611	0.9959	0.9848	0.9947	
	CS/UG/RS/VS1/ $\gamma=251\%$	2.101	0.537	0.9976	0.9785	0.9746	
	CS/UG/RS/VS1/ $\gamma=730\%$	1.129	0.422	0.9845	0.9444	0.8389	
	CS/UG/RS/VS1/ $\gamma=1430\%$	0.729	0.500	0.9992	0.9981	0.8800	
	CS/UG/RS/VS1/ $\gamma=2780\%$	0.579	0.472	0.9955	0.9955	0.8373	
	CS/UG/RS/VS1/ $\gamma=2860\%$	0.556	0.458	0.9989	0.9988	0.8179	
	CS/UG/RS/VS1/ $\gamma=11030\%$	0.444	0.467	0.9984	0.9979	0.8280	
	CS/UG/RS/VS1/ $\gamma=11100\%$	0.496	0.480	0.9976	0.9965	0.8641	
	CS/UG/RS/VS2/ $\gamma=285\%$	3.235	0.750	0.9994	0.9855	0.9982	
	CS/UG/RS/VS2/ $\gamma=1180\%$	1.742	0.626	0.9996	0.9924	0.9888	
	CS/UG/RS/VS2/ $\gamma=3350\%$	1.325	0.496	0.9894	0.9691	0.9181	
	CS/UG/RS/VS2/ $\gamma=10920\%$	1.343	0.406	0.9905	0.9388	0.7373	
	CS/UG/RS/VS2/ $\gamma=13280\%$	0.931	0.507	0.9952	0.9906	0.9154	
	CS/UG/RS/VS2/ $\gamma=26650\%$	1.343	0.522	0.9943	0.9779	0.9388	
	CS/UG/RS/VS3/ $\gamma=9040\%$	5.126	0.877	0.9892	0.9626	0.9979	
	CS/UG/RS/VS3/ $\gamma=23900\%$	3.908	0.593	0.9900	0.9224	0.9736	
	CS/UG/RS/VS3/ $\gamma=31700\%$	3.960	0.623	0.9894	0.9283	0.9782	
CS/UG/RS/VS3/ $\gamma=37500\%$	3.062	0.475	0.9964	0.9111	0.9371		
CS/UG/RS/VS3/ $\gamma=147000\%$	3.137	0.495	0.9852	0.8863	0.9248		
Bard (1993)	PC/UG/1DC/ VS=5MPa	1.278	0.793	0.9989	0.9982	0.9980	0.9946
	PC/UG/1DC/ VS=7.5MPa	0.836	0.793	0.9976	0.9906	0.9923	0.9950
	PC /UG/1DC/ VS=10MPa	0.723	0.722	0.9982	0.9896	0.9871	0.9935
	PC /UG/1DC/ VS=20MPa	0.471	0.676	0.9945	0.9635	0.9737	0.9932
	PC /UG/1DC/ VS=40MPa	0.245	0.677	0.9945	0.9091	0.9649	0.9935
	PC /UG/1DC/ VS=57MPa	0.135	0.695	0.9958	0.8569	0.9618	0.9894
	PC /UG/1DC/ VS=100MPa	0.123	0.726	0.9953	0.8238	0.9729	0.9906
Russell & Khalili (2004)	QS/NG (initial)	1.478	1.731	0.9912	0.9022	0.8804	0.9908 0.9768 0.9757 0.9702 0.9896 0.9815
	QS/NG/DT/MES=410kPa	1.044	2.939	0.9944	0.8711	0.8805	
	QS/NG/DT/MES=760kPa	1.090	2.283	0.9930	0.8893	0.8939	
	QS/NG/DT/MES=1417kPa	0.975	2.071	0.9944	0.8946	0.9117	
	QS/NG/DT/MES=2395kPa	0.874	1.741	0.9957	0.8890	0.9242	
	QS/NG/DT/MES=3006kPa	0.873	1.547	0.9953	0.9022	0.9393	
	QS/NG/DT/MES=5705kPa	0.760	1.306	0.9959	0.8983	0.9573	
	QS/NG/DT/MES=7800kPa	0.666	1.204	0.9967	0.8859	0.9657	
Zhang et al. (2017)	ST/NG (initial)	1.666	1.185	0.9745	0.9598	0.9342	0.9908 0.9768 0.9757 0.9702 0.9896 0.9815
	ST/NG/1DC/VS=2MPa	1.304	1.139	0.9742	0.9680	0.9657	
	ST/NG/1DC/VS=5MPa	0.977	1.121	0.9823	0.9561	0.9759	
	ST/NG/1DC/VS=10MPa	0.883	0.845	0.9902	0.9719	0.9949	
	ST/NG/1DC/VS=15MPa	0.771	0.763	0.9839	0.9701	0.9913	
	ST/NG/1DC/VS=20MPa	0.689	0.733	0.9857	0.9594	0.9897	
	SM/NG (initial)	2.351	0.991	0.9879	0.9905	0.9612	
	SM/NG/1DC/VS=2MPa	1.336	0.958	0.9778	0.9822	0.9832	
	SM/NG/1DC/VS=5MPa	0.826	0.914	0.9903	0.9556	0.9913	
	SM/NG/1DC/VS=10MPa	0.657	0.755	0.9835	0.9565	0.9905	
	SM/NG/1DC/VS=15MPa	0.512	0.682	0.9887	0.9617	0.9866	
	SM/NG/1DC/VS=20MPa	0.406	0.787	0.9969	0.9066	0.9959	
Xiao et al.	CS/UG/IL/SH1, IW=4.71KJ	1.808	0.669	0.9982	0.9895	0.9867	0.9922

(2016)	CS/UG/IL/SH1, IW=9.71KJ	1.454	0.527	0.9940	0.9773	0.9309	0.9808
	CS/UG/IL/SH1, IW=19.42KJ	1.105	0.433	0.9856	0.9709	0.8371	0.9538
	CS/UG/IL/SH1, IW=38.85KJ	0.644	0.438	0.9827	0.9830	0.786	0.9079
	CS/UG/IL/SH2, IW=4.71KJ	2.851	0.818	0.9873	0.9650	0.9871	0.9965
	CS/UG/IL/SH2, IW=9.71KJ	2.490	0.683	0.9820	0.9447	0.9632	0.9921
	CS/UG/IL/SH2, IW=19.42KJ	2.157	0.569	0.9795	0.9224	0.917	0.9796
	CS/UG/IL/SH2, IW=38.85KJ	1.890	0.514	0.9760	0.9079	0.8707	0.9666
	CS/UG/IL/SH3, IW=4.71KJ	3.351	1.070	0.9914	0.9819	0.9971	0.9990
	CS/UG/IL/SH3, IW=9.71KJ	3.145	0.897	0.9811	0.9597	0.9859	0.9966
	CS/UG/IL/SH3, IW=19.42KJ	2.924	0.814	0.9763	0.9473	0.9758	0.9918
	CS/UG/IL/SH3, IW=38.85KJ	2.637	0.715	0.9746	0.9347	0.9603	0.9860
	CS/UG/IL/SH3, IW=4.71KJ	3.566	1.208	0.9932	0.9863	0.9981	0.9995
	CS/UG/IL/SH3, IW=9.71KJ	3.449	1.060	0.9839	0.9711	0.9920	0.9980
	CS/UG/IL/SH3, IW=19.42KJ	3.298	0.969	0.9801	0.9624	0.9874	0.9967
CS/UG/IL/SH3, IW=38.85KJ	3.125	0.895	0.9780	0.9556	0.9828	0.9951	
Mayoraz et al. (2006)	ST/UG/ML/MMP=0.5MPa	3.348	1.059	0.9872	0.9799	0.9922	
	ST/UG/ML/MMP=1MPa	1.872	0.463	0.9806	0.9114	0.8608	
	ST/UG/ML/MMP=3MPa	0.748	0.300	0.9902	0.9246	0.4546	
	LT/UG/ML/MMP=0.5MPa	3.870	1.587	0.9990	0.9984	0.9996	
	LT/UG/ML/MMP=1MPa	3.522	1.321	0.9998	0.9989	0.9991	
	LT/UG/ML/MMP=3MPa	2.027	0.842	0.9990	0.9987	0.9985	

- 2 Note: CS-Carbonate Sand, PC-Petroleum Coke, QS-Quartz Sand, SM-Sandy Mudstone, ST-Sandstone, LT-
3 Limestone
4 UG-uniformly graded, NG-non-uniformly graded
5 RS-Ring shear test, 1DC-One dimensional compression, DT-Drained triaxial test, IL-Impact loading test, ML-
6 Monotonic loading test
7 VS-vertical stress, VS1-vertical stress ranges 650–930 kPa, VS2-vertical stress ranges 248–386kPa, VS3-vertical
8 stress ranges 60–97kPa, MES- mean effective stress, MMP-maximum mean pressure
9 SH1-specimen height=31.8mm, SH2-specimen height=63.7mm, SH3-specimen height=95.5mm, SH4-specimen
10 height=127.3mm, IW-input work
11
12